Chemical Engineering Journal 275 (2015) 351–356

Contents lists available at ScienceDirect

Chemical Engineering Journal

journal homepage: www.elsevier.com/locate/cej

NO oxidation over Ni–Co perovskite catalysts

Shifa Zhong, Yuanyuan Sun, Hongchuan Xin *, Chunpeng Yang, Lei Chen, Xuebing Li

Key Laboratory of Biofuels, Qingdao Institute of Bioenergy and Bioprocess Technology, Chinese Academy of Sciences, Qingdao 266101, China

HIGHLIGHTS

- Co-precipitation method to prepare $LaNi_{1-x}Co_xO_3$.
- $LaNi_{0.7}Co_{0.3}O_3$ shows superior catalytic activity to other $LaNi_{1-x}Co_xO_3$ catalysts.
- Cost-effective and catalytically efficient catalyst for NO oxidation.
- Moderate amount of adsorbed NO and O_2 and moderate adsorption strength both contribute to high reactivity.

GRAPHICAL ABSTRACT

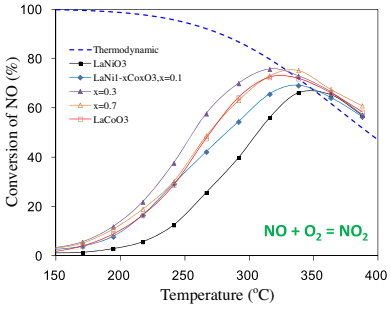

ARTICLE INFO

Article history:
Received 20 February 2015
Received in revised form 8 April 2015
Accepted 10 April 2015
Available online 16 April 2015

Keywords:
NO
Ni–Co perovskite
Co-precipitation
Catalytic oxidation

ABSTRACT

$LaNi_{1-x}Co_xO_3$ (x = 0, 0.1, 0.3, 0.7, 1.0) perovskite catalysts were prepared by co-precipitation method and investigated in the catalytic oxidation of NO. $LaNi_{0.7}Co_{0.3}O_3$ showed the best catalytic activity among all the samples, confirming the potential of $LaNi_{0.7}Co_{0.3}O_3$ as a cheap and efficient NO oxidation catalyst. The high reactivity of $LaNi_{0.7}Co_{0.3}O_3$ was mainly due to the moderate amount of adsorbed NO and O_2 and their moderate adsorption strength on the surface of the catalyst, as determined by the XRD, H_2-TPR, NO-TPD, O_2-TPD and XPS studies.

1. Introduction

Vehicular engines operating under lean burn conditions are becoming more and more popular because of their higher fuel efficiency and thus lower CO_2 emission than conventional Otto gasoline engines. However, because excess O_2 is used in these vehicles, the traditional three-way catalysts are ineffective for NO_x treatment. The NO_x emitted from the exhausts have manyfold devastating effects on the atmosphere and ecosystems (such as ozone layer depletion, photochemical smog and acid rain) and also on human health. Hence, it is a challenge for researchers to remove NO_x from this oxidizing environment.

Two of the most promising technologies for reducing NO_x under the oxygen-rich environment are ammonia selective catalytic reduction (NH_3-SCR) and lean NO_x trap (LNT). In the fast NH_3-SCR process, two main reactions contribute to NO_x conversion by ammonia:

$$2NO + O_2 = 2NO_2 \quad (1)$$

$$2NH_3 + NO + NO_2 = 2N_2 + 3H_2O \quad (2)$$

The NO:NO_2 ratio of 1:1 is most effective for NO_x reduction for fast SCR catalysts [1]. In the LNT system, during lean operation conditions (i.e., in an oxidizing gas mixture), the NO is firstly oxidized to NO_2 and subsequently stored in the Ba component, while during fuel-rich conditions (i.e., in a reducing gas mixture), the NO_2 is reduced to N_2 and then released to the atmosphere [2]. In these

* Corresponding author.
E-mail address: xinhc@qibebt.ac.cn (H. Xin).

http://dx.doi.org/10.1016/j.cej.2015.04.046
1385-8947/

systems, a pre-catalyst for the oxidation of NO is set before adding the reductant to improve the efficiency of reductant. Hence, it is of great significance to develop the NO oxidation catalysts for practical applications.

For NO oxidation, the platinum-based catalysts have been commonly used. Després et al. found that Pt/SiO_2 (2.5 wt.%) could convert about 80% of NO to NO_2 at 300 °C (reaction conditions: 500 ppm NO-10% O_2) [3]. However, the use of Pt is accompanied with its high cost and poor thermal stability under highly oxidizing conditions. Lira et al. observed that PtO_x species could form on the surface of Al_2O_3, thus lowering the activity of NO oxidation [4]. Consequently, there are substantial interests in the development of better performing, low-cost, and more durable NO oxidation catalysts [5,6]. As we all know, perovskite-based catalysts have been found to be the promising substitutes of Pt-based catalysts due to their ease of synthesis, low cost, and high thermal stability [7,8]. The perovskite oxides have a general formula of ABO_3, where A designates a rare-earth or alkaline earth cation and B a transition metal cation. They have drawn particular interests in that their redox catalytic properties can be easily tuned by substituting a small fraction of A or B site with other cations [9]. Among the perovskite oxides, $LaCoO_3$, $LaMnO_3$ and their doped modifications have been investigated extensively because of their high activities for NO oxidation. The A site substituted perovskite based on $LaCoO_3$ or $LaMnO_3$ can enhance the activity highly compared to un-doped ones. Wen et al. observed the high activities of Ce-doped perovskite catalysts ($La_{1-x}Ce_xCoO_3$) for the oxidation of NO [10]. Kim et al. reported that Sr-doped perovskite ($La_{0.9}Sr_{0.1}CoO_3$) catalyst revealed a superior NO oxidation activity compared to Pt-based catalysts [11]. Shen et al. found that $La_{0.9}Ca_{0.1}MnO_3$ perovskite exhibited high activity for NO oxidation and could convert 82% of NO at 300 °C [12]. Yoon et al. studied $La_{0.8}Ag_{0.2}MnO_3$ with the best activity for NO oxidation among the $La_{1-x}Ag_xMnO_3$ catalysts [13]. However, for NO oxidation, the B site doped perovskites are rarely reported. Wang et al. reported that the highest conversion of NO could be obtained on $LaMn_{0.9}Co_{0.1}O_3$ among the Co-doped $LaMnO_3$ catalysts [14].

$LaNiO_3$ perovskite was mainly used in catalysis of syngas production [15], but seldom employed in NO oxidation. In this work, we investigated the activity of $LaNiO_3$ for NO oxidation and observed that the efficiency of $LaNiO_3$ was unsatisfactory comparing to that of $LaCoO_3$. However, nickel was cheaper than cobalt, making nickel more attractive from the viewpoint of industrial application. Hence, for the purpose of lowering the cost of catalysts and enhancing the catalytic activity of $LaNiO_3$ concurrently, we prepared Co-doped modified $LaNiO_3$ ($LaNi_{1-x}Co_xO_3$) by co-precipitation method and then tested their catalytic activity for NO oxidation. We extensively investigated the effect of Co substitution into the $LaNiO_3$ on the oxidation of NO to NO_2. The roles of Co in the NO oxidation mechanism over the $LaNi_{1-x}Co_xO_3$ were examined by XRD, N_2 adsorption, H_2-TPR, NO-TPD, O_2-TPD and XPS studies.

2. Experimental

2.1. Catalysts preparation

The materials used in the synthesis were metal nitrates and all reagents were purchased from Aladdin. The $LaNi_{1-x}Co_xO_3$ (x = 0, 0.1, 0.3, 0.7, 1.0) catalysts were prepared by co-precipitation method according to a previous report [16]. $La(NO_3)_3{\cdot}6H_2O$, $Ni(NO_3)_2{\cdot}6H_2O$ and $Co(NO_3)_2{\cdot}6H_2O$ were used as precursors. Take the $LaNi_{0.9}Co_{0.1}O_3$ sample as an example, to an aqueous solution containing the metal nitrates as the precursors at a molar ratio of 1 $La(NO_3)_3{\cdot}6H_2O$: 0.9 $Ni(NO_3)_2{\cdot}6H_2O$:0.1 $Co(NO_3)_2{\cdot}6H_2O$, 2 mol/L–1 mol/L NaOH–Na_2CO_3 aqueous solution was added dropwise under magnetic stirring until the pH value reached 10. After that, the resulting suspension was aged for 4 h at room temperature, filtered and washed thoroughly with the deionized water. The obtained precipitate was dried at 120 °C overnight and calcined at 750 °C for 5 h in a muffle furnace, yielding the perovskite catalysts.

2.2. Catalysts characterization

Powder X-ray diffraction (XRD) measurements were performed on a Bruker AXS D8 Focus diffractometer with Cu Kα radiation (40 kV, 40 mA, λ = 1.5406 Å, scanning step = 0.02°) and the diffraction patterns were recorded in the range of $20 < 2\theta < 80°$ at the scanning rate of 6° min^{-1}. Nitrogen adsorption at low temperature (−196 °C) was performed on a Micromeritics ASAP 2020M surface area and porosity analyzer. The specific surface area (SSA) was obtained by Brunauer–Emmett–Teller (BET) method. The catalyst redox behaviors were examined by hydrogen temperature programmed reduction (H_2-TPR). Experiments were conducted on a Micromeritics Autochem 2920 instrument. Prior to each run, the sample (0.1 g) was pre-treated in Ar stream at 200 °C for 30 min. After cooling down to 50 °C, 10% H_2/Ar mixture gas of 20 mL/min was introduced and the reactor was heated at a temperature rate of 10 °C/min from room temperature to 900 °C and maintained at this temperature for 20 min. In NO temperature-programmed desorption (NO-TPD) experiment, the catalyst (1 g) was pretreated in N_2 at 400 °C for 1 h followed by cooling down to 50 °C. After purging with N_2 for 30 min, the gas flow was switched to 400 ppm NO with N_2 balance. After the adsorption was completed, pure N_2 was introduced. The sample was then heated up to 500 °C at a rate of 5 °C/min with pure N_2 (1.3 L/min). The effluent gas was analyzed by the MRU air emission monitoring systems equipped with electrochemical sensors. Oxygen temperature-programmed desorption (O_2-TPD) experiments were performed in a quartz reactor with a TCD as detector. In each analysis, the sample (0.2 g) was pretreated with Ar gas at 200 °C for 1 h. After cooling down to 50 °C, the 5% O_2/Ar mixture gas (20 mL/min) was introduced and the catalyst was purged for 3 h. After the adsorption was completed, pure Ar was charged. The sample was then heated up to 1000 °C at a rate of 15 °C/min. The X-ray photoelectron spectroscopy (XPS) analysis was performed on a VG-Scientific ESCALAB 220iXL spectrometer equipped with a Mg Kα X-ray source ($h\nu$ = 1253.6 eV). The binding energies were corrected by the C 1s peak of carbon at 284.9 eV.

2.3. Catalytic activity test

The NO oxidation activity of perovskite catalysts was examined in a fixed-bed flow reactor. A gas mixture of 400 ppm NO and 6% O_2 in N_2 balance was fed into the reactor system at total flow 1.7 L/min. Prior to each test, the catalyst was pretreated with 6% O_2 in N_2 balance and at 400 °C for 1 h. A physical mixture of a perovskite catalyst (1.0 g, 0.5 mL, 60–80 mesh) and quartz grains (1.0 g, 60–80 mesh) with a particle size of 0.18–0.25 mm was charged into the cylindrical quartz tube reactor (25 mm o.d.), while the GHSV was maintained at 200,000 h^{-1}. The reactants and reactive products were analyzed online by the MRU air emission monitoring systems equipped with electrochemical sensors. The conversion of NO oxidation into NO_2 is defined as the percentage of NO feed that has reacted, i.e.:

$$X(\%) = \frac{NO_{in} - NO_{out}}{NO_{in}} \times 100$$

3. Results and discussion

3.1. Structural characterization

The structural characteristics of the Co-doped perovskite were firstly examined by XRD measurements. As shown in Fig. 1(A), all samples with the typical perovskite structure were successfully obtained with the co-precipitation method, indicating that the co-precipitation method was efficient for preparing perovskite as previous reports [17]. The peak at $2\theta = 33.3°$ belonged to (104) crystal plane of $LaCoO_3$, as shown in Fig. 1(B). With the decrease of Co content, the peak became less prominent and moved to lower angle. So did the peak at $2\theta = 32.8°$ attributed to (110) crystal plane of $LaCoO_3$. The *d*-spacing of (110) calculated from the XRD patterns were listed in Table 1. With the increase of *x* from 0 to 1, the lattice distance of the (110) plane decreased from 2.7299 Å to 2.7205 Å, indicating that the Co^{3+} ion (0.52 Å) was indeed incorporated into the lattice of the perovskite structure and replaced Ni^{3+} ion (0.56 Å) in B site [18]. However, $LaNi_{0.7}Co_{0.3}O_3$ had the largest *d*-spacing, 2.7315 Å. The average crystalline size of $LaNi_{1-x}Co_xO_3$ gradually increased with the increase of Co content, from 15.9 nm to 64.8 nm, which indicated that the Co-doping could benefit the crystal growth by the method of co-precipitation.

BET results of the catalysts are also shown in Table 1. The specific surface areas (SSA) of $LaNi_{1-x}Co_xO_3$ catalysts were relatively low, about 7–11 m^2/g, which was mainly due to the calcination at the high temperature [18]. It is also notable that the substituted samples had a smaller SSA than $LaNiO_3$ and the reduction was linear with the substitution, which was in accordance with a previous report [19].

Table 1
Physicochemical properties of $LaNi_{1-x}Co_xO_3$ catalysts.

$LaNi_{1-x}Co_xO_3$	Crystalline size (nm)[a]	SSA (m^2/g)	*d* (110)[b] (Å)	*d* (104)[b] (Å)
$x = 0$	15.9	11.1	2.7299	–
$x = 0.1$	35.6	9.5	2.7284	2.6988
$x = 0.3$	48.7	7.7	2.7315	2.6987
$x = 0.7$	64.8	7.2	2.7267	2.6925
$x = 1$	56.4	8.9	2.7205	2.6895

[a] Calculated by Software Jade 5.0.
[b] Calculated by the Bragg formula: $2d\sin\theta = n\lambda$.

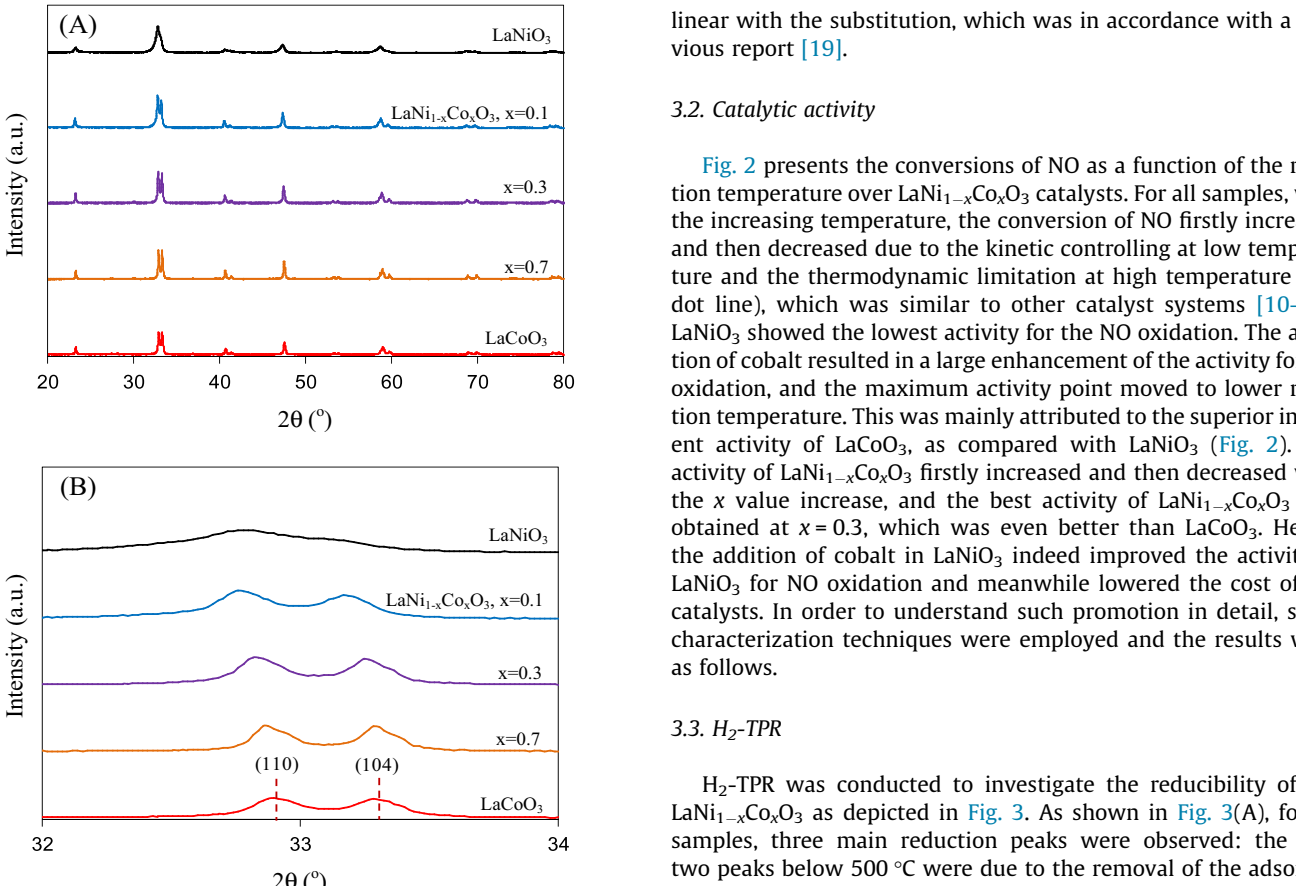

Fig. 1. (A) XRD patterns of $LaNi_{1-x}Co_xO_3$ and (B) partial XRD patterns of all samples in the 2θ range of 32–34°.

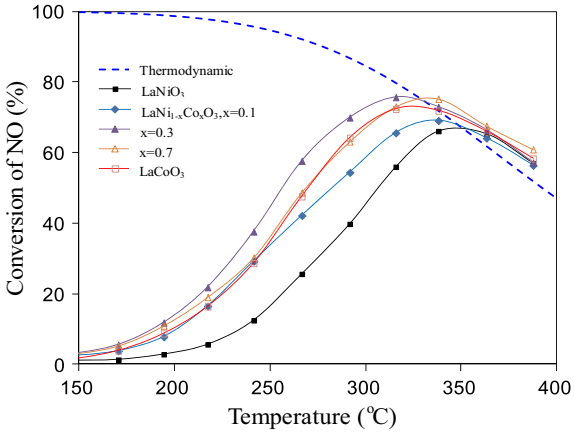

Fig. 2. NO conversion of $LaNi_{1-x}Co_xO_3$ for NO oxidation.

3.2. Catalytic activity

Fig. 2 presents the conversions of NO as a function of the reaction temperature over $LaNi_{1-x}Co_xO_3$ catalysts. For all samples, with the increasing temperature, the conversion of NO firstly increased and then decreased due to the kinetic controlling at low temperature and the thermodynamic limitation at high temperature (the dot line), which was similar to other catalyst systems [10–12]. $LaNiO_3$ showed the lowest activity for the NO oxidation. The addition of cobalt resulted in a large enhancement of the activity for NO oxidation, and the maximum activity point moved to lower reaction temperature. This was mainly attributed to the superior inherent activity of $LaCoO_3$, as compared with $LaNiO_3$ (Fig. 2). The activity of $LaNi_{1-x}Co_xO_3$ firstly increased and then decreased with the *x* value increase, and the best activity of $LaNi_{1-x}Co_xO_3$ was obtained at $x = 0.3$, which was even better than $LaCoO_3$. Hence, the addition of cobalt in $LaNiO_3$ indeed improved the activity of $LaNiO_3$ for NO oxidation and meanwhile lowered the cost of the catalysts. In order to understand such promotion in detail, some characterization techniques were employed and the results were as follows.

3.3. H_2-TPR

H_2-TPR was conducted to investigate the reducibility of the $LaNi_{1-x}Co_xO_3$ as depicted in Fig. 3. As shown in Fig. 3(A), for all samples, three main reduction peaks were observed: the first two peaks below 500 °C were due to the removal of the adsorbed oxygen species on oxygen vacancies with the concomitant reduction of Co^{3+} and Ni^{3+} to Co^{2+} and Ni^{2+}, respectively, and the last peak above 500 °C was attributed to the reduction of Co^{2+} and

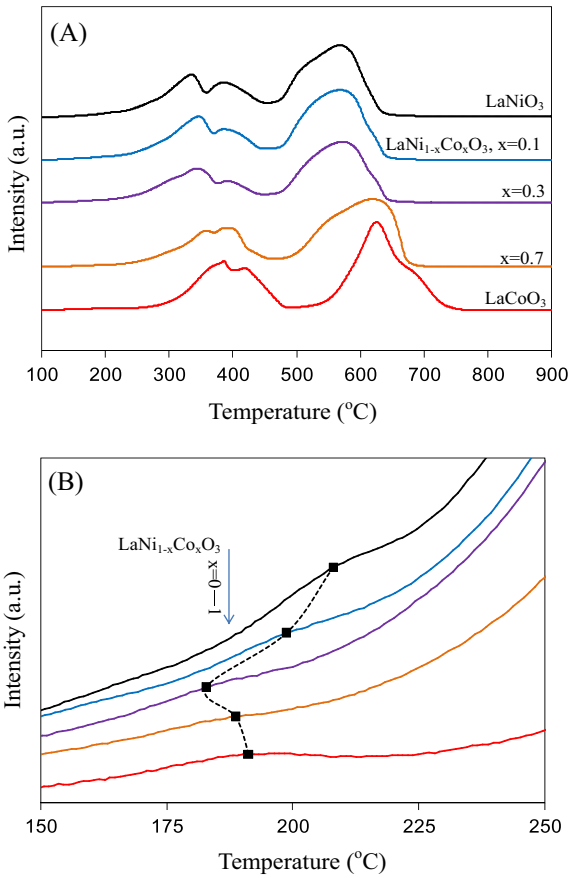

Fig. 3. H_2-TPR profiles of $LaNi_{1-x}Co_xO_3$: (A) temperature at 100–900 °C and (B) temperature at 150–250 °C.

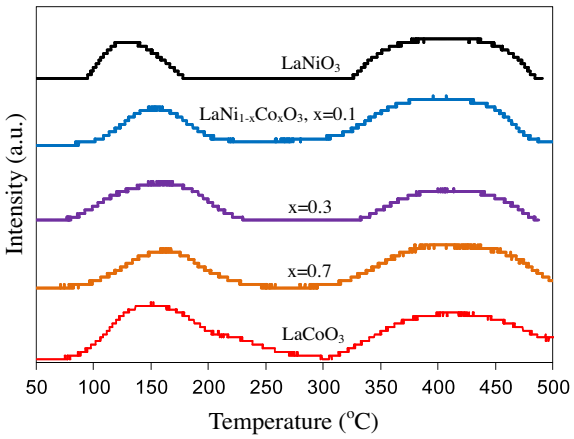

Fig. 4. NO-TPD profiles of $LaNi_{1-x}Co_xO_3$.

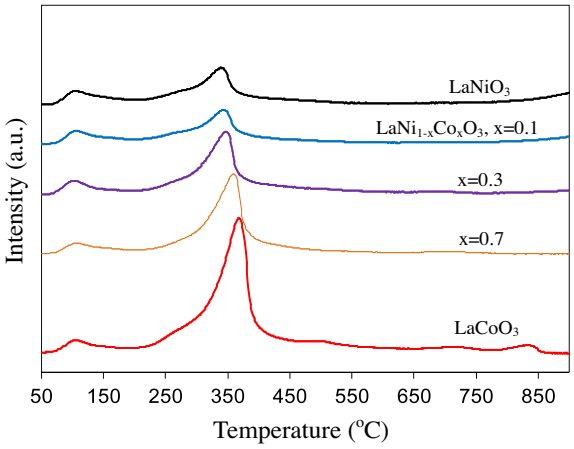

Fig. 5. O_2-TPD profiles of $LaNi_{1-x}Co_xO_3$.

Ni^{2+} to Co^0 and Ni^0, respectively [16,20]. The reduction temperature of $LaCoO_3$ was higher than $LaNiO_3$ in the whole temperature range, so the reduction peaks were gradually shifted to high temperature with the increased content substitution of Ni by Co. This trend was similar with a previous report [18]. The results revealed that $LaNiO_3$ was not as stable as $LaCoO_3$ in the reducing environment and that the Co doping was beneficial for improving the stability of $LaNiO_3$ structure. This was favorable to their application in LNT catalysts, which required frequent exposure to reducing environments during regeneration and/or desulfation processes.

As shown in Fig. 3(B), a small shoulder centered at 150–250 °C appeared, which could be assigned to the reduction of oxygen species adsorbed on the surface [16]. $LaNiO_3$ with the highest reduction temperature showed the lowest activity for NO oxidation. With the increase of doped cobalt content, the reduction temperature was shifted to lower temperature, corresponding to the increased activity for NO oxidation. In the case of $x = 0.3$, the reduction temperature was the lowest, corresponding to the highest activity. When x was increased from 0.3 to 0.7, the reduction temperature was shifted to higher temperature while the amount of oxygen species was decreased, leading to the decreasing activity for NO oxidation. These results may reveal that the oxygen species adsorbed at low temperature may contribute to the activity of NO oxidation.

3.4. NO-TPD

The NO-TPD experiment was conducted to investigate the NO adsorption on the surface of catalysts (Fig. 4). For all samples, there were two main desorption peaks in the whole temperature range: one was at low temperature (<300 °C) and the other was at high temperature (>300 °C). The NO desorbed from the catalysts below 300 °C was ascribed to NO adsorbed at B site in perovskite structure while the NO desorbed above 300 °C was mainly from the decomposition of metal nitro or nitrate on the perovskite surface [21,22]. Compared with $LaCoO_3$, $LaNiO_3$ exhibited lower amount of adsorbed NO and larger distance between two desorption peaks, which indicated that the B site was relevant to NO adsorption [21]. Moreover, Co was superior to Ni for the capability of adsorbing NO, resulting in better performance in NO oxidation. With the increase of Co doping content, the range of desorption temperature of NO became wider, indicating the increased amount of adsorbed NO. However, the amount of NO adsorption was not directly correlated with the NO oxidation activity, which indicated that the amount of NO adsorption was not the only factor to influence the performance of NO oxidation.

3.5. O_2-TPD

In order to directly measure the amount of O_2 adsorbed onto the surface of $LaNi_{1-x}Co_xO_3$, the O_2-TPD measurements were examined, as shown in Fig. 5. Three types of O_2 species were observed over the catalysts employed. The first peak between 50 °C and 150 °C was ascribed to physisorbed oxygen species [23]. The α-O_2 peak (150 °C < T < 500 °C) may be attributed to the oxygen readily desorbed from the surface of $LaNi_{1-x}Co_xO_3$ at relatively low temperatures, whereas the β-O_2 peak (above 500 °C) may

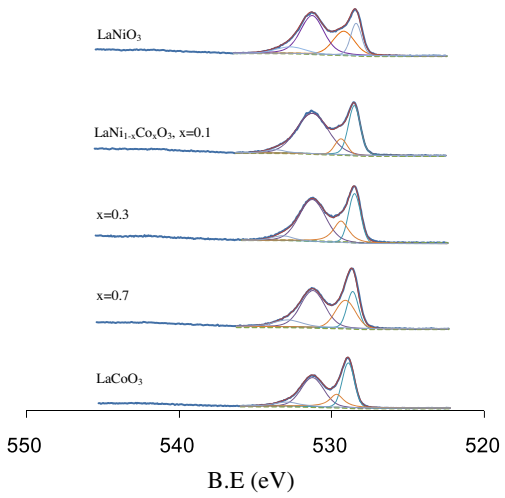

Fig. 6. O 1s XPS spectra of $LaNi_{1-x}Co_xO_3$.

Table 2
XPS results of $LaNi_{1-x}Co_xO_3$ catalysts.

x	La/Co	O_{ads}/O_{total} (%)
0	–	48.4
0.1	9.8	59.4
0.3	4.9	50.4
0.7	2.2	44.0
1.0	1.5	42.5

mainly originate from the bulk [13]. However, the β-O_2 peak became more obvious due to the Co-doping. With the increased content of Co doping, there were two obvious changes observed from the TPD profiles: (i) the content of O_2 desorbed increased gradually, which indicated that the cobalt was superior to nickel for adsorbing O_2 in amount; (ii) the desorption peak was gradually shifted to high temperature, which indicated that the nickel was superior to cobalt for adsorbing O_2 at low temperature. The O_2 desorption temperature represented the adsorption strength on the catalyst surface, and low desorption temperature indicated the weak adsorption of O_2. Hence, the O_2 adsorption strength on nickel was weaker than that on cobalt. The highest activity observed at $x = 0.3$ may be mainly attributed to the adsorbing O_2 with both moderate adsorption strength and proper amount.

3.6. XPS

The $LaNi_{1-x}Co_xO_3$ samples were analyzed by XPS to investigate the element chemical states on the surface of catalysts. As shown in Fig. 6, the O 1s peak was curve-fitted with four peaks: the adsorbed water molecules at 533.5 eV (denoted as O_γ), the adsorbed oxygen at 531.1–531.5 eV (denoted as O_β), the surface lattice oxygen at 529.2 eV (denoted as O_α) and the oxygen species in La_2O_3 at 528.8 eV [10,16]. According to a previous report [24], La_2O_3 was formed easily in the perovskite structure by the co-precipitation method. However, XRD analysis did not reveal the presence of diffraction peaks attributed to lanthanum oxide (La_2O_3) or lanthanum oxycarbonate ($(LaO)_2CO_3$). This could be due to the low quantity of those species on the sample surface. Except for the case when $x = 0.1$, the surface atomic ratios of La/Co were larger than the theoretical ones as shown in Table 2, suggesting the surface enrichment of A-site elements. This phenomenon was commonly observed for perovskite oxides, and no remarkable connection with their catalytic activities could be established [10,16,25]. On the other hand, it is generally accepted that the adsorbed surface oxygen often participates in oxidation reactions. The ratio of O_{ads}/O_{total} was listed in Table 2. With the increased Co dosages, the ratio of O_{ads}/O_{total} firstly increased and then decreased. This could be explained by the results of O_2-TPD: Co was superior to Ni for adsorbing O_2 in amount including the amount of O_{ads}. So Co doping could lead to the increase of O_{ads}/O_{total}; however, the nickel was superior to cobalt for adsorbing O_2 at low temperature, which meant that nickel at the B site was beneficial for adsorbing O_{ads}. Hence, with the increase of Co content, the decrease content of Ni could result in the decrease of O_{ads}/O_{total}. Although the ratio of O_{ads}/O_{total} on $LaNi_{0.9}Co_{0.1}O_3$ sample was the largest among all samples, it did not display the highest activity in NO oxidation. This may result from the lower total amount of oxygen adsorption on $LaNi_{0.9}Co_{0.1}O_3$ as shown in O_2-TPD results (Fig. 5). However, $LaNi_{0.7}Co_{0.3}O_3$ showed not only high ratio of O_{ads}/O_{total} but also proper amount of total oxygen adsorption, resulting in its highest activity for NO oxidation.

4. Conclusion

In summary, the co-precipitation method was appropriate for the formation of perovskite structure. The Co doping at B site in $LaNiO_3$ was beneficial for adsorbing more O_2 and NO, while Ni was in favor of tuning the adsorbed strength of O_2 on the catalysts surface. $LaNi_{0.7}Co_{0.3}O_3$ displayed the best activity among all samples due to the proper amount of adsorbed O_2 and NO and the moderate adsorption strength of O_2. $LaNi_{0.7}Co_{0.3}O_3$ was promising as a cheap and efficient catalyst for NO oxidation.

Acknowledgements

This work was financially supported by the Qingdao Key Technology Program (Nos. 12-1-3-68-nsh, 13-1-3-123-nsh, and 13-4-4-25-chg) and Doctoral Fund of Shandong Province (BS2013CL029).

References

[1] M.F. Irfan, J.H. Goo, S.D. Kim, Co_3O_4 based catalysts for NO oxidation and NO, reduction in fast SCR process, Appl. Catal., B 78 (2008) 267–274.
[2] S. Jeong, S. Youn, D.H. Kim, Effect of Mg/A1 ratios on the NO_x storage activity over Pt–BaO/Mg–Al mixed oxides, Catal. Today 231 (2014) 155–163.
[3] J. Despres, M. Elsener, M. Koebel, O. Krocher, B. Schnyder, A. Wokaun, Catalytic oxidation of nitrogen monoxide over Pt/SiO_2, Appl. Catal., B 50 (2004) 73–82.
[4] E. Lira, L.R. Merte, F. Behafarid, L.K. Ono, L. Zhang, B.R. Cuenya, Role and evolution of nanoparticle structure and chemical state during the oxidation of NO over size- and shape-controlled Pt/gamma-Al_2O_3 catalysts under Operando conditions, ACS Catal. 4 (2014) 1875–1884.
[5] W. Cai, Q. Zhong, W. Zhao, Solvent effects on formation of Cr-doped $Ce_{0.2}Zr_{0.8}O_2$ synthesized with cinnamic acid and their catalysis in oxidation of NO, Chem. Eng. J. 246 (2014) 328–336.
[6] M. Wang, H. Liu, Z.H. Huang, F. Kang, Activated carbon fibers loaded with MnO_2 for removing NO at room temperature, Chem. Eng. J. 256 (2014) 101–106.
[7] R. You, Y. Zhang, D. Liu, M. Meng, Z. Jiang, S. Zhang, Y. Huang, A series of ceria supported lean-burn NO_x trap catalysts $LaCoO_3/K_2CO_3/CeO_2$ using perovskite as active component, Chem. Eng. J. 260 (2015) 357–367.
[8] R.J.H. Voorhoeve, D.W. Johnson, J.P. Remeika, P.K. Gallagher, Perovskite oxides – materials science in catalysis, Science 195 (1977) 827–833.
[9] S. Royer, D. Duprez, F. Can, X. Courtois, C. Batiot-Dupeyrat, S. Laassiri, H. Alamdari, Perovskites as substitutes of noble metals for heterogeneous catalysis: dream or reality, Chem. Rev. 114 (2014) 10292–10368.
[10] Y. Wen, C. Zhang, H. He, Y. Yu, Y. Teraoka, Catalytic oxidation of nitrogen monoxide over $La_{1-x}Ce_xCoO_3$ perovskites, Catal. Today 126 (2007) 400–405.
[11] C.H. Kim, G. Qi, K. Dahlberg, W. Li, Strontium-doped perovskites rival platinum catalysts for treating NO_x in simulated diesel exhaust, Science 327 (2010) 1624–1627.
[12] M. Shen, Z. Zhao, J. Chen, Y. Su, J. Wang, X. Wang, Effects of calcium substitute in $LaMnO_3$ perovskites for NO catalytic oxidation, J. Rare Earth. 31 (2013) 119–123.

[13] D.Y. Yoon, E. Lim, Y.J. Kim, J.H. Kim, T. Ryu, S. Lee, B.K. Cho, I.-S. Nam, J.W. Choung, S. Yoo, NO oxidation activity of Ag-doped perovskite catalysts, J. Catal. 319 (2014) 182–193.
[14] J. Wang, Y. Su, X. Wang, J. Chen, Z. Zhao, M. Shen, The effect of partial substitution of Co in $LaMnO_3$ synthesized by sol–gel methods for NO oxidation, Catal. Commun. 25 (2012) 106–109.
[15] S.-K. Liu, Y.-C. Lin, Generation of syngas through autothermal partial oxidation of glycerol over $LaMnO_3$- and $LaNiO_3$-coated monoliths, Catal. Today 237 (2014) 62–70.
[16] C. Zhang, C. Wang, W. Zhan, Y. Guo, Y. Guo, G. Lu, A. Baylet, A. Giroir-Fendler, Catalytic oxidation of vinyl chloride emission over $LaMnO_3$ and $LaB_{0.2}Mn_{0.8}O_3$ (B = Co, Ni, Fe) catalysts, Appl. Catal., B 129 (2013) 509–516.
[17] C. Zhang, W. Hua, C. Wang, Y. Guo, Y. Guo, G. Lu, A. Baylet, A. Giroir-Fendler, The effect of A-site substitution by Sr, Mg and Ce on the catalytic performance of $LaMnO_3$ catalysts for the oxidation of vinyl chloride emission, Appl. Catal., B 134 (2013) 310–315.
[18] G. Valderrama, M.R. Goldwasser, C.U. de Navarro, J.M. Tatibouet, J. Barrault, C. Batiot-Dupeyrat, F. Martinez, Dry reforming of methane over Ni perovskite type oxides, Catal. Today 107–08 (2005) 785–791.
[19] C.R.B. Silva, L. da Conceicao, N.F.P. Ribeiro, M.M.V.M. Souza, Partial oxidation of methane over Ni–Co perovskite catalysts, Catal. Commun. 12 (2011) 665–668.
[20] O. Gonzalez, J. Lujano, E. Pietri, M.R. Goldwasser, New Co–Ni catalyst systems used for methane dry reforming based on supported catalysts over an INT-MM1 mesoporous material and a perovskite-like oxide precursor $LaCo_{0.4}Ni_{0.6}O_3$, Catal. Today 107–08 (2005) 436–443.
[21] J. Chen, M. Shen, X. Wang, J. Wang, Y. Su, Z. Zhao, Catalytic performance of NO oxidation over $LaMeO_3$ (Me = Mn, Fe, Co) perovskite prepared by the sol–gel method, Catal. Commun. 37 (2013) 105–108.
[22] E. Campagnoli, A. Tavares, L. Fabbrini, I. Rossetti, Y.A. Dubitsky, A. Zaopo, L. Forni, Effect of preparation method on activity and stability of $LaMnO_3$ and $LaCoO_3$ catalysts for the flameless combustion of methane, Appl. Catal., B 55 (2005) 133–139.
[23] N.A. Merino, B.P. Barbero, P. Grange, L.E. Cadus, $La_{1-x}Ca_xCoO_3$ perovskite-type oxides: preparation, characterisation, stability, and catalytic potentiality for the total oxidation of propane, J. Catal. 231 (2005) 232–244.
[24] C. Zhang, Y. Guo, Y. Guo, G. Lu, A. Boreave, L. Retailleau, A. Baylet, A. Giroir-Fendler, $LaMnO_3$ perovskite oxides prepared by different methods for catalytic oxidation of toluene, Appl. Catal., B 148 (2014) 490–498.
[25] M. Alifanti, R. Auer, J. Kirchnerova, F. Thyrion, P. Grange, B. Delmon, Activity in methane combustion and sensitivity to sulfur poisoning of $La_{1-x}Ce_xMn_{1-y}Co_yO_3$ perovskite oxides, Appl. Catal., B 41 (2003) 71–81.